Effects of Imiquimod on Hair Follicle Stem Cells and Hair Cycle Progression

CrossMark

*JID*Open

Nicole Amberg[1], Martin Holcmann[1], Gabriel Stulnig[1] and Maria Sibilia[1]

Topical imiquimod (IMQ) application is widely used as a model for psoriasiform-like skin inflammation in mice. Although the effects on the epidermis are well characterized, it is unclear how IMQ affects hair follicles and cycling. Here we investigated how IMQ affects hair follicle stem cells and whether the timing of IMQ application influences the immune infiltrate. Our results show that IMQ application at mid and late telogen activated hair follicle stem cells leading to premature hair cycle entry (anagen), which was accompanied by massive infiltration of inflammatory macrophages and gamma delta T cells, whereas the number of the respective resident populations decreased. Interestingly, high resident macrophage numbers were present in Rag2$^{-/-}$ mice and were maintained after IMQ treatment explaining why IMQ-induced anagen was reduced. This could be rescued after macrophage depletion suggesting that resident macrophages inhibit whereas inflammatory infiltrating macrophages stimulate hair follicle stem cell activation. The expression of the anagen-inhibiting factor BMP-4 was reduced by IMQ treatment as well as the activating factors Wnt showing that IMQ-induced hair follicle stem cell activation occurs by a Wnt-independent mechanism involving inflammatory cytokines such as CCL2 and TNF-α. On the basis of our findings, we recommend conducting experiments with IMQ during mid and late telogen as the biggest differences in immune cell composition are observed.

INTRODUCTION

Imiquimod (IMQ) is a synthetic immune-response modifier acting as a toll-like receptor 7/8 agonist (Hemmi et al., 2002). In humans, the 5% IMQ cream formulation Aldara is frequently used for the treatment of genital warts, actinic keratosis, and superficial basal cell carcinomas with very high response rates (Bath-Hextall et al., 2014; de Macedo et al., 2015; Gollnick et al., 2005; Peris et al., 2014). In mice and humans, topical application of IMQ results in the activation of the interfollicular epidermis (IFE), upregulation of major histocompatibility complex-II (MHC-II) on keratinocytes, hyperproliferation, and para-keratosis (Flutter and Nestle, 2013), as well as a strong skin inflammation characterized by the infiltration of several immune cells such as plasmacytoid dendritic cells (Drobits et al., 2012; Kalb et al., 2012; Palamara et al., 2004), mast cells (Heib et al., 2007), monocytes (Terhorst et al., 2015), and T cells and activation of the IL-23/IL-17/IL-22 axis (Heib et al., 2007; Riol-Blanco et al., 2014; van der Fits et al., 2009). Langerhans cells (LCs) and gamma delta T cells (gd T cells) are activated in response to IMQ, leading to emigration of LCs (Flacher et al., 2014; Palamara et al., 2004; Pantelyushin et al., 2012). In the past few years, IMQ has been widely used by several researchers as a model for psoriasiform-like skin inflammation (Perera et al., 2014; Schonthaler et al., 2013; Tortola et al., 2012; van der Fits et al., 2009), as, similar to psoriasis, epidermal thickening is induced by IL-22 released from infiltrating immune cells (Van Belle et al., 2012).

Despite IMQ's known effects on the IFE, its effects on hair follicle (HF) and hair follicle stem cells (HFSCs) are unknown. The HF is a highly organized structure and is subdivided into the infundibulum (IF)/junctional zone at the top, the isthmus, the bulge (Bu), and the lowest part, the secondary hair germ (2°HG) (Amberg et al., 2015; Arwert et al., 2012; Jaks et al., 2010). Each of these regions of the HF harbors defined stem cells, which under homeostatic conditions serve to renew their compartment. Following HF morphogenesis after birth, renewal of the HF occurs in a largely synchronized manner (hair cycle) in the mouse until 90 days after birth and is divided into three stages, the resting phase (telogen), active phase (anagen), and destructive phase (catagen). Toward the end of telogen, quiescent stem cells from the 2°HG and later from the whole Bu become activated and proliferate to initiate anagen to generate new hair (Blanpain and Fuchs, 2009; Fuchs, 2007). At the end of anagen, progenitor cells and transit-amplifying cells stop proliferating and undergo apoptosis (catagen), leading to HF shortening and entrance into the quiescent telogen phase (Greco et al., 2009; Ito et al., 2004; Mesa et al., 2015; Tumbar et al., 2004).

[1]Institute of Cancer Research, Department of Medicine I, Comprehensive Cancer Center, Medical University of Vienna, Vienna, Austria

Correspondence: Maria Sibilia, Institute of Cancer Research, Department of Medicine I, Comprehensive Cancer Center, Medical University of Vienna, Borschkegasse 8a, A-1090 Vienna, Austria. E-mail: maria.sibilia@meduniwien.ac.at

Abbreviations: Bmp, bone morphogenetic protein; Bu, bulge; DETC, dendritic epidermal T cells; gd T cells, gamma delta T cells; HF, hair follicle; 2°HG, secondary hair germ; HFSC, hair follicle stem cell; IF, infundibulum; IFE, interfollicular epidermis; IMQ, imiquimod; LCs, Langerhans cells; MHC-II, major histocampatibility complex-II; P, postnatal day; TNFα, tumor necrosis factor-α
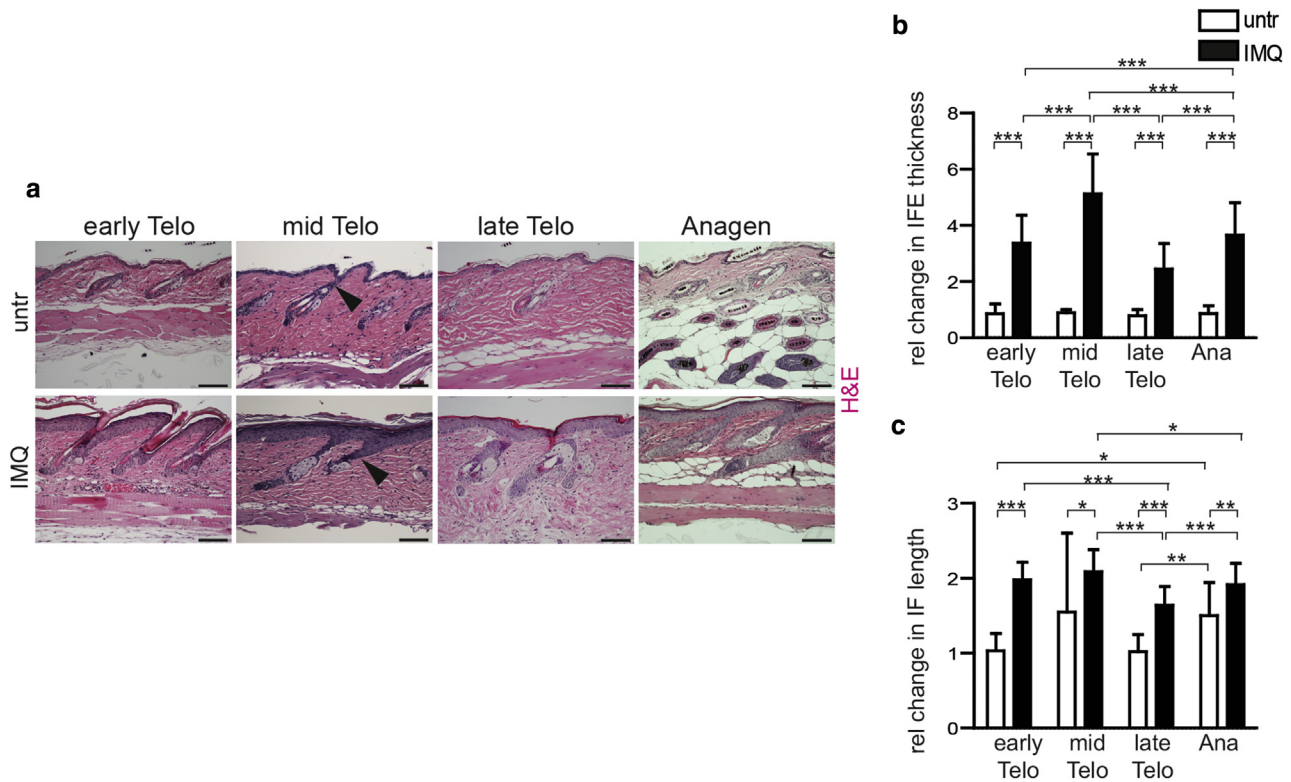
Figure 1. Imiquimod (IMQ) treatment during late telogen induces hair follicle stem cell activation. (**a**) Representative images of hematoxylin and eosin (H&E) stainings of back skin sections from mice treated with or without IMQ at indicated time points. Black arrows indicate the infundibulum (IF). Scale bar: 100 μm. Quantification of (**b**) the thickness of the interfollicular epidermis (IFE) and (**c**) the length of the IF at indicated time points and treatments.

HFSC activity is highly controlled, not only by stem cell-derived factors, which can be either inhibitory or activating, but also by immune cell- or other dermal cell-derived factors, such as Bmp2, Bmp4, Wnt10, Dkk1, follistatin, noggin, Sfrp4, and TNFα (Botchkarev, 2001; Castellana et al., 2014; Chen et al., 2014, 2015; Plikus et al., 2008). Because IMQ leads to infiltration of different immune cell populations into the skin, it is very likely that they affect HFSC and hair cycle progression. Recently, it was shown that HF cells are responsive to immune cells, such as macrophages, which under steady-state conditions produce factors either inhibiting (e.g., Bmp4) or activating (e.g., Wnts) HFSCs, depending on the telogen stage (Castellana et al., 2014). Upon depletion of skin-resident macrophages by clodronate-mediated apoptosis, the activating factors were released and HFs entered anagen. Also dendritic epidermal T cells (DETC) and dermal mast cells were shown to be present at different concentrations during the distinct hair cycle stages, emphasizing that there is crosstalk between HFs and immune cells (Maurer et al., 1995, 1997; Paus et al., 1994).

In this study, we aimed at investigating the effects of IMQ on HF and whether IMQ-induced immune responses are affected during the different hair cycle stages. Because IMQ is a widely used model of skin inflammation to study psoriasis-like skin diseases, these parameters are important to consider when planning experiments with IMQ to guarantee and increase reproducibility and avoiding variances between different laboratories.

RESULTS

IMQ treatment during late telogen induces HF stem cell activation and premature hair cycle entry

Experiments with topical IMQ are usually performed with 6- to 12-week-old mice when the second and third hair cycle occur. We therefore investigated whether IMQ application results in different effects on the skin when applied at different stages of the hair cycle. Wild-type C57BL/6 mice were shaved on the dorsum and 1 day later topically treated with Aldara for 7 consecutive days starting either at postnatal day 50 (P50) (early telogen), at P57 (mid telogen), at P65 (late telogen), or at P80 (anagen) (see Supplementary Figure S1a online). All IMQ-treated mice responded to treatment irrespective of the hair cycle stage, as indicated by the increase in spleen size, which results from a systemic inflammatory response that is typically observed in mice after Aldara treatment (see Supplementary Figure S1b) (Palamara et al., 2004). IFE thickness and IF length (taken as a readout for skin inflammation) were increased to various degrees by IMQ treatment during the different hair cycle stages (Figure 1a−c). The increase in IFE diameter was lowest in mice receiving IMQ treatment in late telogen, whereas it was comparable during early telogen and anagen (Figure 1b). IF length already revealed differences in untreated mice and was significantly increased in anagen when compared with the other stages (Figure 1c).

We next analyzed whether IMQ also activates 2°HG and HF Bu stem cells by performing immunofluorescence staining for the epidermal-dermal boundary marker β4
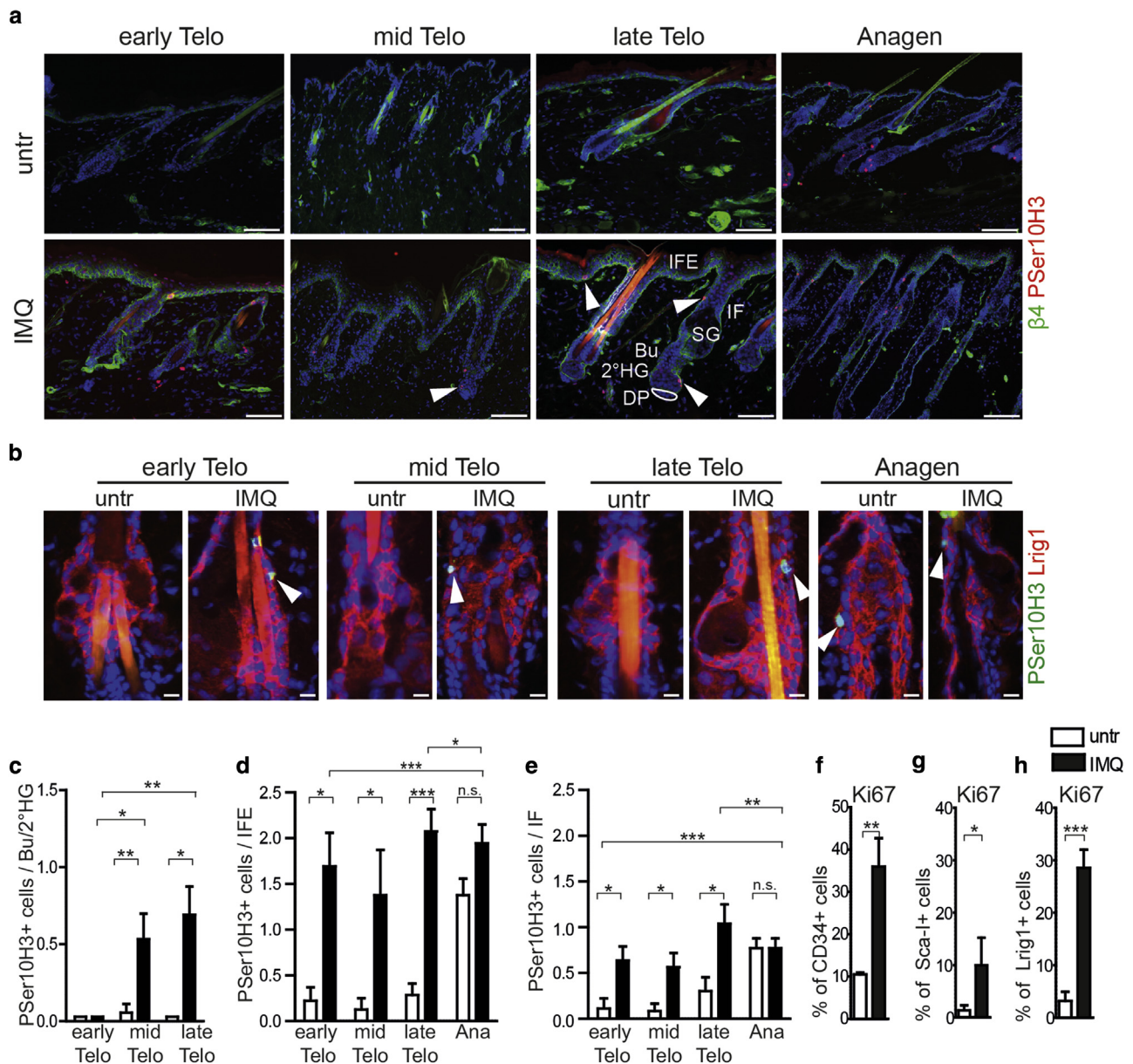
Figure 2. Imiquimod (IMQ) application induces proliferation in distinct epidermal compartments. (**a, b**) Stainings of back skin sections from mice of indicated treatment and time points. (**a**) β4 integrin (A488, green), PSer10H3 (A594, red), nuclei (Hoechst, blue). The white arrows point at PSer10H3$^+$ nuclei in different epidermal compartments, and the white ellipse indicates dermal papilla (DP). Bu, bulge; 2°HG, secondary hair germ; IF, infundibulum; IFE, interfollicular epidermis; SG, sebaceous gland. Scale bar: 100 μm. (**b**) Lrig1 (red), PSer10H3 (green), nuclei (blue). The white arrows point at PSer10H3$^+$ nuclei. Scale bar: 100 μm. (**c–e**) Quantification of numbers of PSer10H3$^+$ cells in (**c**) Bu/2°HG, (**d**) IFE, and (**e**) IF at indicated time points and treatments. FACS analysis showing the percentages of Ki67$^+$ cells in (**f**) integrin α6$^+$ CD34$^+$ bulge cells, (**g**) Sca-I$^+$ IFE cells, and (**h**) Lrig1$^+$ IF cells.

integrin together with the M-phase marker PSer10H3 (Figure 2a). These cells are usually quiescent during telogen and are therefore PSer10H3-negative. IMQ treatment during early telogen had no effect on HFSC activation, because we did not observe PSer10H3$^+$ cells in the 2°HG or Bu (Figure 2a and c). Interestingly, IMQ treatment during mid and late telogen revealed a profound increase in PSer10H3$^+$ cells in the 2°HG and Bu, leading to identification of premature anagen entry in up to 90% of all HFs investigated (Figure 2a and c). We also determined the number of cells in mitosis in IFE and IF, by counting PSer10H3$^+$ cells either in the β4 integrin$^+$ fraction of the epidermis (Figure 2a) or in the

Lrig1$^+$ fraction that labels the IF (Figure 2b, see Supplementary Figure S1c). IMQ treatment during early telogen increased proliferation of keratinocytes in the IFE and the IF, but not in the 2°HG (Figure 2c–e). In contrast, during mid and late telogen, the proliferation was enhanced in all three compartments. However, IMQ application during anagen did not alter proliferation of IFE and IF compared with untreated mice (Figure 2c–e). We were able to confirm these results by additionally performing Ki67 staining (see Supplementary Figure S1d), demonstrating precocious HFSC activation when mice received IMQ treatment during mid and late telogen (see Supplementary Figure S1e).
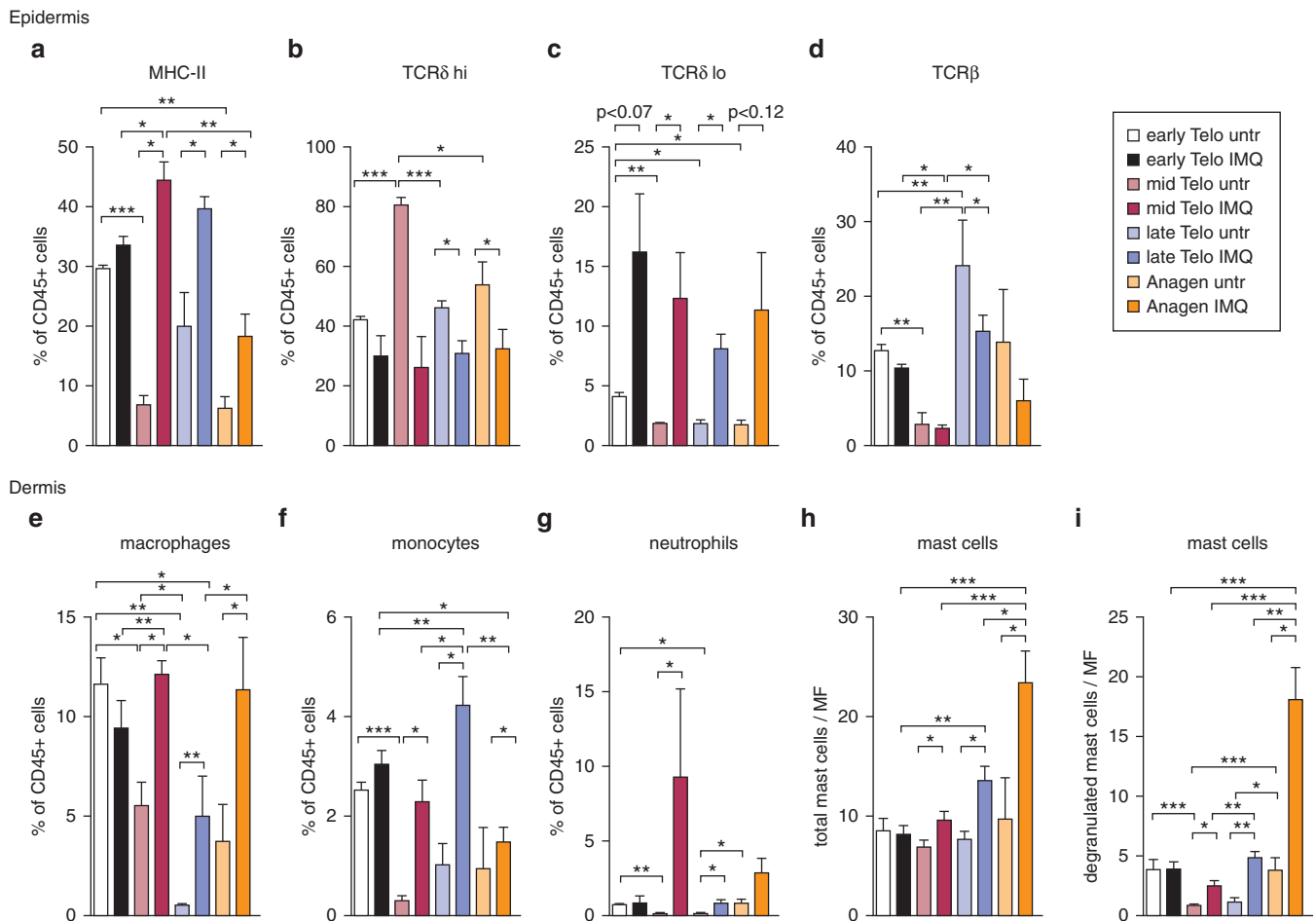
Figure 3. Effects of imiquimod (IMQ) treatment on skin immune cells. FACS analysis of epidermal suspensions isolated from mice treated or not with IMQ at indicated time points, showing the percentage of (**a**) MHCII$^+$ cells, (**b**) TCRδ^{hi} cells, (**c**) TCRδ^{lo} cells, and (**d**) TCRβ$^+$ cells of CD45$^+$ cells. FACS analysis of dermal cell suspensions isolated from mice treated or not with IMQ at indicated time points, showing the percentage of (**e**) macrophages (F4/80$^+$) of CD45$^+$ cells, (**f**) infiltrating monocytes (Ly6C^{hi}) of CD11b$^+$ cells within the CD45$^+$ population, and (**g**) neutrophils (Ly6G^{hi} Ly6C$^+$) cells of CD11b$^+$ cells within the CD45$^+$ population. Quantification of the number of (**h**) total mast cells and (**i**) degranulated mast cells per microscopic field (MF) at indicated time points and treatments. MHC, major histocompatibility complex. TCR, T cell receptor.

Closer analysis with known stem cell markers for the Bu (α6 Integrin^{hi} CD34$^+$), IFE (α6 Integrin$^+$ Sca-I^{hi}), and IF (α6 Integrin$^+$ Lrig1$^+$) by flow cytometry (FACS) analysis at late telogen revealed increased percentages of Ki67$^+$ cells within each of these cell compartments in IMQ-treated mice (Figure 2f–h, see Supplementary Figure S1f–h). Taken together, these results demonstrate that IMQ treatment has different effects on the HFSC compartment depending on the hair cycle stage, in particular, leading to increased stem cell proliferation and premature entry into anagen when applied at mid and late telogen.

Effects of IMQ treatment on the skin immune cell composition during hair cycle

Because topical IMQ treatment also leads to a prominent infiltration of immune cells into the skin, we next analyzed the composition of the cutaneous inflammatory infiltrate during the four hair cycle stages. FACS analysis of epidermal cell suspensions (Supplementary Figure S2a online) revealed a comparable activation of keratinocytes by IMQ at all stages, as defined by MHC-II expression in CD45$^-$ cells (see

Supplementary Figure S2c). There was also a trend toward an increase in the total number of immune cells (CD45$^+$) in IMQ-treated epidermis at each time point (see Supplementary Figure S2d). Interestingly, the relative number of MHC-II$^+$ immune cells in the epidermis of untreated mice, which are mainly LCs, was lower in mid telogen and anagen and increased when IMQ was applied in mid and late telogen, as well as anagen (Figure 3a). In contrast, in untreated skin, the percentage of DETC (TCRδ^{hi}) was significantly higher in mid telogen and anagen (Figure 3b). IMQ treatment decreased the numbers of TCRδ^{hi} cells irrespective of the time of application (Figure 3b). However, after IMQ treatment, the number of TCRδ^{lo} γδ T cells, the majority of which are most likely infiltrating from the periphery, significantly increased at all stages (Figure 3c). We were also able to detect TCRβ$^+$ cells in the epidermis, which were highest during late telogen and decreased after IMQ treatment (Figure 3d). FACS analysis of dermal cell suspensions (see Supplementary Figure S2b) showed that the percentages of CD45$^+$ cells fluctuated between the distinct hair cycle stages, with significantly more leukocytes in the dermis of untreated anagen mice, which
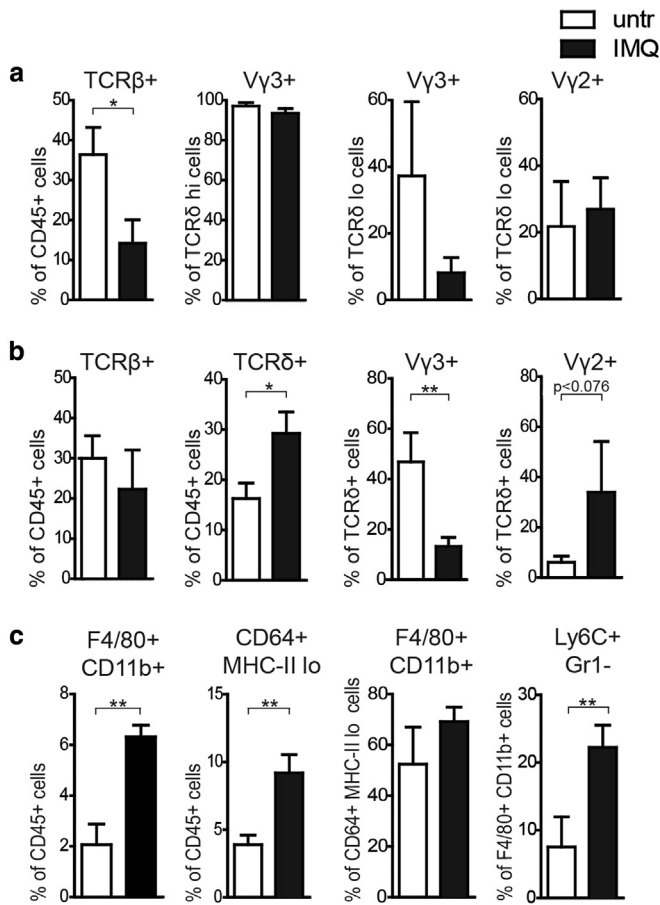
Figure 4. Imiquimod (IMQ) treatment leads to infiltration of inflammatory γδ T cells and macrophages. FACS analysis of (**a**) epidermal and (**b, c**) dermal cell suspensions isolated from mice treated or not with IMQ at late telogen, showing the percentage of (**a**) TCRβ$^+$ cells of CD45$^+$ cells, Vγ3$^+$ cells of TCRδ^{hi} cells, and Vγ3$^+$ cells and Vγ2$^+$ cells of TCRδ^{lo} cells; (**b**) TCRβ$^+$ cells of CD45$^+$ cells, TCRδ$^+$ cells of CD45$^+$ cells and Vγ3$^+$ cells, and Vγ2$^+$ cells of TCRδ$^+$ cells; (**c**) F4/80$^+$ CD11b$^+$ cells of CD45$^+$ cells, CD64$^+$ MHC-II^{lo} cells of CD45$^+$ cells, F4/80$^+$ CD11b$^+$ cells of CD64$^+$ MHC-II^{lo} cells, and Ly6C$^+$ GR1$^-$ cells of F4/80$^+$ CD11b$^+$ cells. MHC, major histocompatibility complex. TCR, T cell receptor.

decreased after IMQ application (see Supplementary Figure S2e). Closer inspection of the CD45$^+$ cell compartment revealed remarkable differences in macrophages (F4/80$^+$ CD11c$^-$), monocytes (CD11b$^+$ Ly6C^{hi}), and neutrophils (CD11b$^+$ Ly6G^{hi} Ly6C$^+$) (Figure 3e–g). In line with a previous report (Castellana et al., 2014), in untreated skin macrophage ratios decreased from early to late telogen, thus allowing anagen transition (Figure 3e). A similar trend was observed for neutrophils and monocytes (Figure 3f and g). Importantly, IMQ treatment during mid and late telogen and anagen, but not in early telogen, induced infiltration of macrophages, neutrophils, and monocytes (Figure 3e–g).

We next quantified mast cells using Giemsa staining, because they express toll-like receptor 7 and were shown to be implicated in topical IMQ response (see Supplementary Figure S2f) (Heib et al., 2007). Total number of mast cells did not change after IMQ treatment during early telogen and mast cells were also not activated, as evidenced by the number of degranulated mast cells (Figure 3h and i).

However, when IMQ was applied during mid and late telogen as well as anagen, the number of mast cells and their activation state significantly increased. This effect was strongest after IMQ application during anagen (Figure 3h and i).

These results demonstrate that except for mast cells, which remain constant during the whole hair cycle, in untreated skin, all other myeloid cells (macrophages, neutrophils, and monocytes) decrease during the transition from early to late telogen and increase again in anagen. Moreover, except for TCRδ^{lo} γδ T cells, IMQ treatment had no significant effects on the composition of the immune infiltrate of the skin when applied during early telogen. In contrast, during all other hair cycle stages, IMQ application significantly increased the number of all myeloid cells including mast cells and TCRδ^{lo} γδ T cells, whereas the numbers of other T-cell populations in the epidermis decreased.

IMQ treatment leads to infiltration of inflammatory γδ T cells and macrophages

Because T cells had been shown to play a crucial role in IMQ-mediated skin inflammation (Pantelyushin et al., 2012), and declining macrophage numbers were shown to favor anagen induction (Castellana et al., 2014), we sought to characterize both cell populations in more detail.

Within the epidermal T-cell populations, we detected TCRβ$^+$ cells in untreated mice, which decreased on IMQ-induced skin inflammation (Figure 4a, see Supplementary Figure S3a online). These epidermal TCRβ$^+$ cells are predominantly memory T cells, as shown by expression of CD8α, CD69, and CD103 (Supplementary Figure S3b) (Heath and Carbone, 2013). Detailed investigation of the epidermal γδ T-cell population showed that TCRδ^{hi} expressing cells were exclusively DETC, as demonstrated by expression of Vγ3 (Figure 4a, see Supplementary Figure S3a), whereas TCRδ^{lo} expressing cells were both DETC and infiltrating Vγ2$^+$ T cells (Figure 4a, see Supplementary Figure S3a, nomenclature according to Garman et al., 1986). In the dermis, TCRβ$^+$ cell numbers did not significantly change after IMQ application; however, γδ T-cell populations did, as reported previously (Figure 4b, see Supplementary Figure S3c) (Pantelyushin et al., 2012). Whereas in untreated mice, the majority of dermal γδ T cells expressed Vγ3, on IMQ treatment we detected a strong infiltrate of Vγ2$^+$ T cells that have recently been shown to be key mediators of IMQ-induced psoriasiform skin inflammation (Figure 4b, see Supplementary Figure S3c) (Gray et al., 2013).

In the dermis of IMQ-treated mice, we found an increased percentage of F4/80$^+$ CD11b$^+$ cells, which are mainly macrophages. Dendritic cells could be excluded from this population by staining for CD64$^+$ MHC-II^{lo} cells, which were increased after IMQ treatment and mainly consisted of F4/80$^+$ CD11b$^+$ macrophages (Figure 4c and Supplementary Figure S3d). Importantly, we detected an increase of Ly6C$^+$ Gr1$^-$ cells within the macrophage population (F4/80$^+$ CD11b$^+$) in IMQ-treated skin, providing evidence that the increase in dermal macrophages may be derived from infiltrating monocytes rather than proliferation of skin-resident macrophages (Figure 4c).
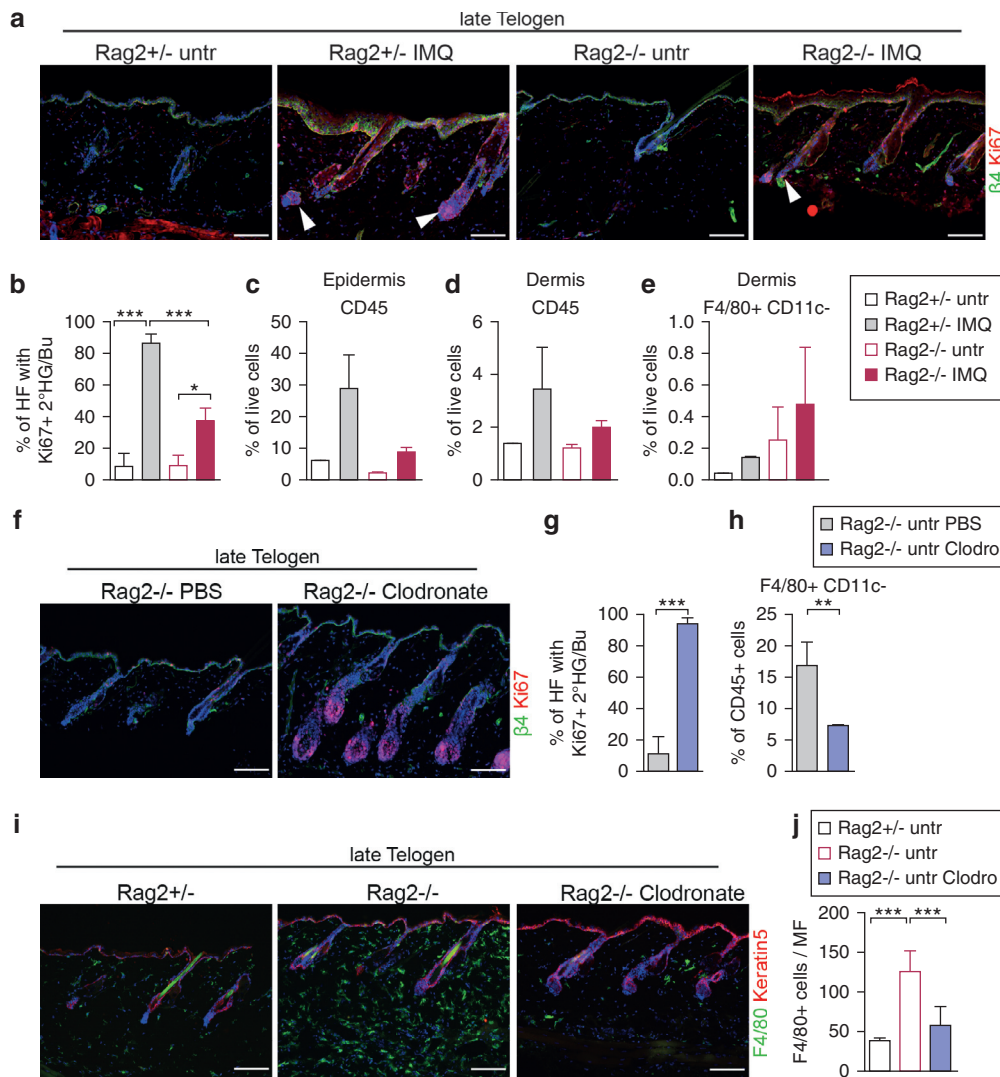
Figure 5. Macrophages, but not T cells, appear to regulate hair follicle stem cell (HFSC) activity. (a) Stainings for β4 integrin (green), Ki67 (red), and nuclei (blue) from mice of indicated genotypes and treatments. (b) Quantification of anagen hair follicle (HF) from mice of indicated genotypes and treatments. FACS analysis showing (c) CD45$^+$ cells of live epidermal cells (d), CD45$^+$ cells of live dermal cells, and (e) F4/80$^+$ cells of live dermal cells. (f) Stainings for β4 integrin (green), Ki67 (red), and nuclei (blue). (g) Quantification of anagen HF from Rag2$^{-/-}$ mice of indicated treatments. (h) Dermal FACS analysis showing F4/80$^+$ cells of CD45$^+$ cells. (i) Stainings for F4/80 (green), keratin 5 (red), and nuclei (blue) from mice of indicated genotypes and treatments. (j) Quantification of macrophage numbers per microscopic field (MF) from mice of indicated genotypes and treatments. All scale bars 100 μm.

Macrophages and T cells regulate HFSC activity

We next investigated which immune cells might be causative for IMQ-induced anagen induction. To investigate the role of T cells in IMQ-induced anagen induction, we treated T- and B-cell-deficient Rag2$^{-/-}$ mice (see Supplementary Figure S4a online) with IMQ during late telogen and monitored hair cycle entry by Ki67 staining (Figure 5a). Surprisingly, in IMQ-treated Rag2$^{-/-}$ mice, only 40% of HFs were in anagen, which was significantly lower than what was observed in control Rag2$^{+/-}$ HF, where 90% of HFs had entered anagen (similar to what was observed with C57BL/6 in Supplementary Figure S1e) (Figure 5b). To our surprise, FACS analysis of immune cells from epidermal and dermal cell suspensions (Figure 5c–e) revealed that—when compared with Rag2$^{+/-}$ mice—untreated Rag2$^{-/-}$ mice displayed already elevated numbers of F4/80$^+$ cells in the dermis with a tendency to increase further after IMQ treatment (Figure 5e and i). This finding led us to speculate whether the high number of macrophages might prevent efficient anagen entry after IMQ treatment. We therefore depleted skin-resident macrophages by subcutaneous clodronate liposome injection (Supplementary Figure S4b) at late telogen. In wild-type

mice, this resulted in anagen induction in almost 100% of all HFs (see Supplementary Figure S4c–e), similar to what was observed in a previous report (Castellana et al., 2014). Moreover, no changes in epidermal and dermal CD45$^+$ immune cell numbers could be seen (see Supplementary Figure S4f and g). Interestingly, macrophage depletion fully restored the capacity of Rag2$^{-/-}$ HF to enter anagen (Figure 5f–j). Immunofluorescence staining for F4/80 revealed a broad distribution of the high number of F4/80$^+$ cells within the dermis of Rag2$^{-/-}$ mice, which was restored to control levels after chlodronate treatment (Figure 5i and j). These data suggest that in the absence of T and B cells increased numbers of dermal macrophages are present in the dermis, which prevent efficient anagen entry after IMQ treatment.

IMQ treatment shifts the balance of HFSC inhibitory and activating factors

In search of a possible mechanism by which IMQ regulates HF activity, we analyzed the expression of candidate growth factors known to be activating (e.g., Wnt3a and Wnt7b) or inhibiting (e.g., Bmp4) anagen entry (Castellana et al., 2014;
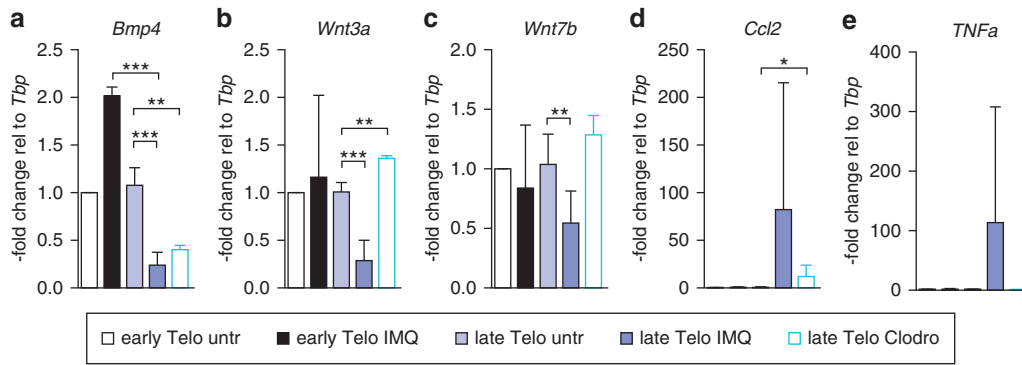
Figure 6. Imiquimod (IMQ) treatment shifts the balance of hair follicle stem cell (HFSC) inhibitory and activating factors. qRT-PCR data obtained from whole skin lysates of mice of indicated time points and treatments, showing results for (**a**) *Bmp4*, (**b**) *Wnt3a*, (**c**) *Wnt7b*, (**d**) *Ccl2*, and (**e**) *TNFα*. Bmp4, bone morphogenetic protein-4; qRT-PCR, quantitative real-time reverse transcription-PCR; TNFα, tumor necrosis factor-α; CCL2, chemokine (C-C Motif) ligand 2; Wnt, wingless-related integration site; Tbp, TATA binding protein.

Kandyba et al., 2013; Plikus et al., 2008). Quantitative real-time reverse transcription-PCR analysis performed on total skin lysates revealed that IMQ treatment leads to an increase in Bmp4 expression during early telogen, but to reduced Bmp4 levels during late telogen. Also macrophage depletion during late telogen by clodronate treatment decreased Bmp4 expression levels similar to what was observed after IMQ application (Figure 6a), showing that downregulation of inhibitory factors is required for anagen entry. Interestingly, the levels of Wnt3a and Wnt7b, which similar to a previous report (Castellana et al., 2014) were found to be increased after clodronate treatment, were not upregulated by IMQ (Figure 6b and c). To our surprise, these factors significantly decreased after IMQ treatment in late telogen, suggesting that IMQ-induced anagen occurs by a different mechanism that does not require Wnt upregulation.

Therefore, we looked at the expression of inflammatory cytokines such as CCL2 and TNFα that had previously been reported to be involved in precocious anagen induction after injury (Chen et al., 2015). Both these cytokines were barely detectable in the skin of untreated mice, and upregulated after IMQ treatment during late telogen, but not during early telogen (Figure 6d and e). These data suggest that after IMQ treatment infiltrating macrophages produce proinflammatory cytokines that stimulate HFSC activation.

DISCUSSION
Most experiments with topical IMQ are performed in mice aged 6−12 weeks. This time window covers different hair cycle stages: early telogen (7−8 weeks), mid telogen (8−9 weeks), late telogen (9−10 weeks), and anagen (10−11 weeks), which might differently affect the response to IMQ. Our data suggest that the composition of the immune infiltrate and the activation state of different epidermal stem cells changes according to the different hair cycle stages. We show activation of stem cells located in the 2°HG when IMQ is applied during mid and late telogen with rapid anagen induction. As telogen can be divided into a refractory (when hair is not responsive to activating cues) and competent (when hair is responsive) phase (Plikus et al., 2008), with refractory telogen lasting

approximately 28 days, it is intriguing that IMQ can overcome refractivity of telogen during the second hair cycle and initiate anagen.

Previous studies reported that besides the dermal papilla, dermal fibroblasts and adipocytes as well as skin-resident dermal macrophages can produce important factors such as Bmp4, Wnt3a, and Wnt7b, which regulate HFSC activity (Castellana et al., 2014; Fuchs, 2007; Plikus et al., 2008). Moreover, dermal resident macrophages were shown to express IL-10 under a steady-state condition, thus playing an anti-inflammatory and scavenging role in the skin (Tamoutounour et al., 2013). However, under inflammatory conditions, monocyte-derived macrophages infiltrate the skin and support the production of cytokines such as TNFα, IL-6, IL-12, and IFNs (Chen et al., 2015; Drobits et al., 2012; Morimura et al., 2016; Terhorst et al., 2015). Injury-induced CCL2 production by the skin was recently shown to induce macrophage infiltration and TNFα production, ultimately resulting in hair cycle induction (Chen et al., 2015). Such macrophages have been shown to be derived from Ly6C$^+$ cells from the blood (Willenborg et al., 2012). In line with this, we can demonstrate CCL2 and TNFα production in mice treated with IMQ during late telogen, which is accompanied by macrophage influx, thus providing evidence that also in the IMQ model, inflammatory macrophages favor hair cycle entry by production of cytokines. Interestingly, depletion of skin-resident macrophages using clodronate during the steady-state also leads to precocious anagen induction, which might seem paradoxical. However, it needs to be emphasized that steady-state resident macrophages analyzed in the clodronate experiment are very different from infiltrating inflammatory macrophages, which differentiate from circulating monocytes. These two cell populations most likely have different functions, and it is therefore not surprising that they secrete a different repertoire of cytokines.

We find that in both conditions (clodronate depletion and IMQ treatment) precocious anagen induction is accompanied by reduced expression of Bmp4, a growth factor that has been shown to inhibit the telogen-anagen transition and anagen progression (Botchkarev, 2001). However, we did not find increased levels of Wnt3a and Wnt7b in IMQ-treated

skin during late telogen like it has been observed after clodronate depletion of resident macrophages. It is possible that activated macrophages infiltrating the skin after IMQ treatment might be able to activate HFSC by a Wnt-independent mechanism. However, it is important to note that we performed our expression analysis in total skin lysates. Therefore, we cannot formally exclude that around the HF there is a local increase of Wnt concentration. Moreover, IMQ-induced infiltration of macrophages and other immune cells leads to a cytokine storm able of activating HFSC, which might be associated with the dilution of Wnt mRNA derived from resident macrophages. Recent studies have shown that Wnt3a mediates anti-inflammatory effects leading to reduced TNFα and IL-6 levels (Neumann et al., 2010; Schaale et al., 2011). These observations support our results, which demonstrate that in early telogen Wnt3a levels are unchanged with no monocytic infiltration, whereas in late telogen Wnt3a is reduced and monocyte influx as well as TNFα levels increased.

CCL2-induced monocyte recruitment and production of TNFα does not seem to happen in early telogen, when high numbers of resident macrophages are present in the dermis already under physiological conditions possibly preventing significant entry of infiltrating macrophages after IMQ treatment. High macrophage numbers are seen in T-cell-deficient Rag2$^{-/-}$ mice already under steady-state conditions and are maintained after IMQ treatment, thus providing an explanation why IMQ-induced anagen is reduced. Only clodronate-mediated depletion of resident macrophages leads to full activation of HFSCs and anagen induction further supporting the conclusion that resident macrophages inhibit whereas inflammatory infiltrating macrophages stimulate anagen induction.

Because our results show remarkable differences in the response of the skin to IMQ treatment between different hair cycle stages, experiments using IMQ should be performed during a defined time window. We recommend applying topical IMQ on murine back skin during mid and late telogen, as significant differences in both HFSC activation and immune cell infiltration can be observed at this stage of the hair cycle. This standardization would allow a better comparison of experiments performed in different laboratories.

MATERIAL AND METHODS

Mice
C57BL/6 and Rag2$^{-/-}$ mice were purchased from Jackson Laboratories and kept in a conventional animal facility of the Medical University of Vienna for several generations in accordance with institutional policies and federal guidelines. Animal experiments were approved by the Animal Experimental Ethics Committee of the Medical University of Vienna and the Austrian Federal Ministry of Science and Research.

Imiquimod treatment
Female and male mice were anesthetized and hair of the back skin was shaved with an electrical small animal razor (Aesculap Favorita II, #GT104, Aesculap, Maria Enzersdorf, Austria) 1 day before starting IMQ (Aldara, Medapharma, Solna, Sweden) treatment for 7 days. Visual inspection of the shaved back skins was performed to confirm the hair cycle stage of the mice. For telogen experiments,

dark pigmentation and associated signs of hair regrowth on the back skin led to exclusion of the respective mice; for anagen experiments, the absence of dark pigmentation on the back skin led to exclusion of the respective mice, according to Plikus et al. (2008). Around 30 mg of Aldara per mouse was used: 1 day after the last IMQ application mice were killed and their back skin was analyzed.

Macrophage depletion
Anesthetized mice were shaved on their back skin at P63 and 50 µl of liposomes either packed with phosphate buffered saline or clodronate (Encapsula Nanosciences, Brentwood, TN) were injected subcutaneously in the anterior and posterior dorsum. Liposomes were a generous gift of Luigi Tortola. Liposome injection was repeated every other day. At P65, IMQ was topically applied to the back skin for 7 consecutive days. One day after the last IMQ application, mice were killed and back skin was analyzed.

Histology
Paraffin sections and cryosections were prepared as previously described (Amberg et al., 2015). Briefly, 4-µm paraffin sections were stained with hematoxylin and eosin (Sigma-Aldrich, Vienna, Austria) or Giemsa (Merck, Vienna, Austria) according to standard procedures. Six-micrometer frozen sections were subjected to immunofluorescence stainings, using 4% paraformaldehyde (PFA) (Merck) fixation for 10 minutes, followed by blocking with 1% BSA (Sigma), 5% Horse Serum (Life Technologies, Darmstadt, Germany), and 0.1% Triton X-100 (Merck) in phosphate buffered saline (Sigma). Antibodies were diluted in blocking buffer and incubated over night at 4 °C. Sections were incubated with secondary antibodies (Life Technologies, 1:500) and Hoechst (Sigma, 1 µg/ml) for 1 hour at room temperature and mounted (DAKO, Vienna, Austria). Antibodies employed are listed in Supplementary Table S1 online.

Epidermal thickness and IF length were measured from hematoxylin and eosin stained sections by taking at least 10 photographs per sample with a ×20 objective at a Nikon eclipse i80 microscope. From each image, epidermal thickness was measured in three different areas. Mast cell quantification was performed from Giemsa stainings by taking at least 10 photographs per sample with a ×20 objective. Both epidermal thickness measurement and mast cell counting were performed using Adobe Photoshop PS5.

Flow cytometry
For immune cell analysis, dermal and epidermal cell suspensions were isolated according to previous publications (Glitzner et al., 2014; Holcmann et al., 2009). After separating epidermis and dermis, cell suspensions were filtered and stained with fluorescently labeled antibodies after blocking with Fc-block (BD Pharmingen, Schwechat, Austria). Antibodies are listed in Supplementary Table S1.

For Ki67 analysis, epidermal cell suspensions were isolated by incubating the back skin dermal side down on 0.25 mg/ml thermolysin (thermolysin powder, Sigma, dissolved in DMEM) over night (O.N.) at 4 °C. Next day, epidermis was gently peeled of and minced. Cell suspensions were filtered and stained with fluorescently labeled antibodies after blocking with Fc-block (BD Pharmingen, Schwechat, Austria). For intracellular staining, we first used Zombie Aqua fixable dead cell staining dye (BioLegend, San Diego, CA) according to the manufacturer's instructions and then followed the fixation and permeabilization protocol of the BD BrdU flow kit (BD Biosciences), and finally 5 µl of Ki67 antibody was added to each sample for 30 minutes at 4 °C. All antibodies are

listed in Supplementary Table S1. Data were acquired on a Fortessa flow cytometer (BD Biosciences) and analyzed using FlowJo (Treestar, Ashland, OR).

Quantitative real-time reverse transcription-PCR

A piece of back skin was surgically removed from the anterior part of the shaved back skin part, added to a tube containing 200 μl of RNALater (Applied Biosystems, Foster City, CA), snap frozen in liquid nitrogen, and stored at −80 °C until further use. For RNA isolation, skin was transferred to a Precellys tube (Peqlab, Erlangen, Germany) containing 1 ml of trizol (Sigma) and homogenized using a Precellys 24 homogenizer (Peqlab) at 2−3 cycles for 2 minutes. RNA was extracted following the standard protocol for chloroform/isopropanol precipitation. One hundred micrograms of RNA were used for reverse transcription, using M-MuLV reverse transcriptase (New England Biolabs, Ipswich, MA) and random hexamers (Invitrogen, Carlsbad, CA). cDNA was stored at −20 °C until further use. Quantitative real-time reverse transcription-PCR was run with SYBR green (Peqlab) on an ABI7500 quantitative real-time reverse transcription-PCR machine (Applied Biosystems). Data were calculated relatively to expression of reference gene Tbp. Primer sequences were ordered from MWG Eurofins (Ebersberg, Germany) and can be found in Supplementary Table S2 online.

Statistical analysis

Data were analyzed by two-tailed Student's t test. Error bars represent ±SD of at least two pooled independent experiments, unless otherwise stated. P values less than 0.05 were considered statistically significant. $*P < 0.05$, $**P < 0.005$, $***P < 0.001$.

SUPPLEMENTARY MATERIAL
Supplementary material is linked to the online version of the paper at www.jidonline.org, and at http://dx.doi.org/10.1016/j.jid.2016.06.613.

REFERENCES

Amberg N, Holcmann M, Glitzner E, Novoszel P, Stulnig G, Sibilia M. Mouse models of nonmelanoma skin cancer. In: Eferl R, Casanova E, editors. Mouse Models of Cancer. Methods in molecular biology, vol. 1267. Springer Science + Business Media; 2015. p. 217−50.

Arwert EN, Hoste E, Watt FM. Epithelial stem cells, wound healing and cancer. Nat Rev Cancer 2012;12:170−80.

Bath-Hextall F, Ozolins M, Armstrong SJ, Colver GB, Perkins W, Miller PS, et al. Surgical excision versus imiquimod 5% cream for nodular and superficial basal-cell carcinoma (SINS): a multicentre, non-inferiority, randomised controlled trial. Lancet Oncol 2014;15:96−105.

Blanpain C, Fuchs E. Epidermal homeostasis: a balancing act of stem cells in the skin. Nat Rev Mol Cell Biol 2009;10:207−17.

Botchkarev VA. Noggin is required for induction of the hair follicle growth phase in postnatal skin. FASEB J 2001;15:2205−14.

Castellana D, Paus R, Perez-Moreno M. Macrophages contribute to the cyclic activation of adult hair follicle stem cells. PLoS Biol 2014;12:e1002002.

Chen C-C, Murray PJ, Jiang TX, Plikus MV, Chang Y-T, Lee OK, et al. Regenerative hair waves in aging mice and extra-follicular modulators follistatin, Dkk1, and Sfrp4. J Invest Dermatol 2014;134:2086−96.

Chen CC, Wang L, Plikus MV, Jiang TX, Murray PJ, Ramos R, et al. Organ-level quorum sensing directs regeneration in hair stem cell populations. Cell 2015;161:277−90.

de Macedo EM, Carneiro RC, de Lima PP, Silva BG, Matayoshi S. Imiquimod cream efficacy in the treatment of periocular nodular basal cell carcinoma: a non-randomized trial. BMC Ophthalmol 2015;15:35.

Drobits B, Holcmann M, Amberg N, Swiecki M, Grundtner R, Hammer M, et al. Imiquimod clears tumors in mice independent of adaptive immunity by converting pDCs into tumor-killing effector cells. J Clin Invest 2012;122:575−85.

Flacher V, Tripp CH, Mairhofer DG, Steinman RM, Stoitzner P, Idoyaga J, et al. Murine Langerin+ dermal dendritic cells prime CD8+ T cells while Langerhans cells induce cross-tolerance. EMBO Mol Med 2014;6:1191−204.

Flutter B, Nestle FO. TLRs to cytokines: mechanistic insights from the imiquimod mouse model of psoriasis. Eur J Immunol 2013;43:3138−46.

Fuchs E. Scratching the surface of skin development. Nature 2007;445:834−42.

Garman RD, Doherty PJ, Raulet DH. Diversity, rearrangement, and expression of murine T cell gamma genes. Cell 1986;45:733−42.

Glitzner E, Korosec A, Brunner PM, Drobits B, Amberg N, Schonthaler HB, et al. Specific roles for dendritic cell subsets during initiation and progression of psoriasis. EMBO Mol Med 2014;6:1312−27.

Gollnick H, Barona CG, Frank RG, Ruzicka T, Megahed M, Tebbs V, et al. Recurrence rate of superficial basal cell carcinoma following successful treatment with imiquimod 5% cream: interim 2-year results from an ongoing 5-year follow-up study in Europe. Eur J Dermatol 2005;15:374−81.

Gray EE, Ramirez-Valle F, Xu Y, Wu S, Wu Z, Karjalainen KE, et al. Deficiency in IL-17-committed Vgamma4(+) gammadelta T cells in a spontaneous Sox13-mutant CD45.1(+) congenic mouse substrain provides protection from dermatitis. Nat Immunol 2013;14:584−92.

Greco V, Chen T, Rendl M, Schober M, Pasolli HA, Stokes N, et al. A two-step mechanism for stem cell activation during hair regeneration. Cell Stem Cell 2009;4:155−69.

Heath WR, Carbone FR. The skin-resident and migratory immune system in steady state and memory: innate lymphocytes, dendritic cells and T cells. Nat Immunol 2013;14:978−85.

Heib V, Becker M, Warger T, Rechtsteiner G, Tertilt C, Klein M, et al. Mast cells are crucial for early inflammation, migration of Langerhans cells, and CTL responses following topical application of TLR7 ligand in mice. Blood 2007;110:946−53.

Hemmi H, Kaisho T, Takeuchi O, Sato S, Sanjo H, Hoshino K, et al. Small anti-viral compounds activate immune cells via the TLR7 MyD88-dependent signaling pathway. Nat Immunol 2002;3:196−200.

Holcmann M, Stoitzner P, Drobits B, Luehrs P, Stingl G, Romani N, et al. Skin inflammation is not sufficient to break tolerance induced against a novel antigen. J Immunol 2009;183:1133−43.

Ito M, Kizawa K, Hamada K, Cotsarelis G. Hair follicle stem cells in the lower bulge form the secondary germ, a biochemically distinct but functionally equivalent progenitor cell population, at the termination of catagen. Differentiation 2004;72:548−57.

Jaks V, Kasper M, Toftgard R. The hair follicle-a stem cell zoo. Exp Cell Res 2010;316:1422−8.

Kalb ML, Glaser A, Stary G, Koszik F, Stingl G. TRAIL(+) human plasmacytoid dendritic cells kill tumor cells in vitro: mechanisms of imiquimod- and IFN-alpha-mediated antitumor reactivity. J Immunol 2012;188:1583−91.

Kandyba E, Leung Y, Chen YB, Widelitz R, Chuong CM, Kobielak K. Competitive balance of intrabulge BMP/Wnt signaling reveals a robust gene network ruling stem cell homeostasis and cyclic activation. Proc Natl Acad Sci USA 2013;110:1351−6.

Maurer M, Fischer E, Handjiski B, von Stebut E, Algermissen B, Bavandi A, et al. Activated skin mast cells are involved in murine hair follicle regression (catagen). Lab Invest 1997;77:319−32.

Maurer M, Paus R, Czarnetzki BM. Mast cells as modulators of hair follicle cycling. Exp Dermatol 1995;4:266−71.

Mesa KR, Rompolas P, Zito G, Myung P, Sun TY, Brown S, et al. Niche-induced cell death and epithelial phagocytosis regulate hair follicle stem cell pool. Nature 2015;522:94−7.

Morimura S, Oka T, Sugaya M, Sato S. CX3CR1 deficiency attenuates imiquimod-induced psoriasis-like skin inflammation with decreased M1 macrophages. J Dermatol Sci 2016;82:175—88.

Neumann J, Schaale K, Farhat K, Endermann T, Ulmer AJ, Ehlers S, et al. Frizzled1 is a marker of inflammatory macrophages, and its ligand Wnt3a is involved in reprogramming mycobacterium tuberculosis-infected macrophages. FASEB J 2010;24:4599—612.

Palamara F, Meindl S, Holcmann M, Luhrs P, Stingl G, Sibilia M. Identification and characterization of pDC-like cells in normal mouse skin and melanomas treated with imiquimod. J Immunol 2004;173:3051—61.

Pantelyushin S, Haak S, Ingold B, Kulig P, Heppner FL, Navarini AA, et al. Rorgammat+ innate lymphocytes and gammadelta T cells initiate psoriasiform plaque formation in mice. J Clin Invest 2012;122:2252—6.

Paus R, Hofmann U, Eichmuller S, Czarnetzki BM. Distribution and changing density of gamma-delta T cells in murine skin during the induced hair cycle. Br J Dermatol 1994;130:281—9.

Perera GK, Ainali C, Semenova E, Hundhausen C, Barinaga G, Kassen D, et al. Integrative biology approach identifies cytokine targeting strategies for psoriasis. Sci Transl Med 2014;6:223ra22.

Peris K, Stockfleth E, Gupta G, Aractingi S, Dakovic R, Dirschka T, et al. Efficacy of imiquimod 3.75% from Lmax according to the number of actinic keratosis lesions. J Eur Acad Dermatol Venereol 2014;29:2470—3.

Plikus MV, Mayer JA, de la Cruz D, Baker RE, Maini PK, Maxson R, et al. Cyclic dermal BMP signalling regulates stem cell activation during hair regeneration. Nature 2008;451:340—4.

Riol-Blanco L, Ordovas-Montanes J, Perro M, Naval E, Thiriot A, Alvarez D, et al. Nociceptive sensory neurons drive interleukin-23-mediated psoriasiform skin inflammation. Nature 2014;510:157—61.

Schaale K, Neumann J, Schneider D, Ehlers S, Reiling N. Wnt signaling in macrophages: augmenting and inhibiting mycobacteria-induced inflammatory responses. Eur J Cell Biol 2011;90:553—9.

Schonthaler HB, Guinea-Viniegra J, Wculek SK, Ruppen I, Ximenez-Embun P, Guio-Carrion A, et al. S100A8-S100A9 protein complex mediates psoriasis by regulating the expression of complement factor C3. Immunity 2013;39:1171—81.

Tamoutounour S, Guilliams M, Montanana Sanchis F, Liu H, Terhorst D, Malosse C, et al. Origins and functional specialization of macrophages and of conventional and monocyte-derived dendritic cells in mouse skin. Immunity 2013;39:925—38.

Terhorst D, Chelbi R, Wohn C, Malosse C, Tamoutounour S, Jorquera A, et al. Dynamics and transcriptomics of skin dendritic cells and macrophages in an imiquimod-induced, biphasic mouse model of psoriasis. J Immunol 2015;195:4953—61.

Tortola L, Rosenwald E, Abel B, Blumberg H, Schafer M, Coyle AJ, et al. Psoriasiform dermatitis is driven by IL-36-mediated DC-keratinocyte crosstalk. J Clin Invest 2012;122:3965—76.

Tumbar T, Guasch G, Greco V, Blanpain C, Lowry WE, Rendl M, et al. Defining the epithelial stem cell niche in skin. Science 2004;303:359—63.

Van Belle AB, de Heusch M, Lemaire MM, Hendrickx E, Warnier G, Dunussi-Joannopoulos K, et al. IL-22 is required for imiquimod-induced psoriasiform skin inflammation in mice. J Immunol 2012;188:462—9.

van der Fits L, Mourits S, Voerman JS, Kant M, Boon L, Laman JD, et al. Imiquimod-induced psoriasis-like skin inflammation in mice is mediated via the IL-23/IL-17 axis. J Immunol 2009;182:5836—45.

Willenborg S, Lucas T, van Loo G, Knipper JA, Krieg T, Haase I, et al. CCR2 recruits an inflammatory macrophage subpopulation critical for angiogenesis in tissue repair. Blood 2012;120:613—25.